

1      **Lower Crustal Composition in the Southwestern United**  
2      **States**

3      **L. G. Sammon<sup>1</sup>, C. Gao<sup>1</sup>, W. F. McDonough<sup>1,2</sup>**

4      <sup>1</sup>Department of Geology, University of Maryland, College Park, MD 20742, USA

5      <sup>2</sup>Department of Earth Sciences and Research Center for Neutrino Science, Tohoku University, Sendai  
6      980-8578, Japan

7      **Key Points:**

- 8
- A 3D composition model for the lower crust of the southwestern United States by  
9      combining seismological and geochemical datasets
  - Composition displays lateral variations that follow geologic province boundaries
  - Lower crustal composition transitions gradually from more felsic to more mafic  
11      with increasing depth
- 12

13      **Abstract**

14      The composition of the lower continental crust is well-studied, but poorly under-  
 15      stood because of the difficulty of sampling large portions of it. Petrological and geochem-  
 16      ical analyses of this deepest portion of the continental crust are limited to the study of  
 17      high grade metamorphic lithologies, such as granulite. In situ lower crustal studies re-  
 18      quire geophysical experiments to determine regional-scale phenomena. Since geophys-  
 19      ical properties, such as shear wave velocity ( $V_s$ ), are nonunique among different com-  
 20      positions and temperatures, the most informative lower crustal models combine both geo-  
 21      chemical and geophysical knowledge. We explored a combined modeling technique by  
 22      analyzing the Basin and Range and Colorado Plateau of the United States, a region for  
 23      which plentiful geochemical and geophysical data are available. By comparing seismic  
 24      velocity predictions based on composition and thermodynamic principles to ambient noise  
 25      inversions, we identified three compositional trends in the southwestern United States  
 26      that reflect three different geologic settings. Identifying the composition of the lower crust  
 27      depends heavily on its temperature because of the effect it has on rock mineralogy and  
 28      physical properties. In this region, we see evidence for a lower crust that overall is intermediate-  
 29      mafic in composition ( $53.7 \pm 7.2$  wt.%  $\text{SiO}_2$ ), and notably displays a gradient of decreas-  
 30      ing  $\text{SiO}_2$  with depth.

31      **1 Introduction**

32      The composition of the lower continental crust, despite its influence over crust for-  
 33      mation and geologic hazards, remains a mystery. Though as thin as 10 km in some re-  
 34      gions (Rudnick & Gao, 2003), the lower crust contributes critically to the temperature,  
 35      structure, and stress state of the continent. Lower crustal deformation models are heav-  
 36      ily informed by deep crust silica content, water, and mineralogy (Jackson, 2002). How-  
 37      ever, because of the relative scarcity (<1% of all samples listed on [http://www.EarthChem](http://www.EarthChem.org/)  
 38      .org/)) and the compositional heterogeneity of deep crustal samples, it is difficult to con-  
 39      strain the bulk composition of the lower crust purely through geochemical or petrolog-  
 40      ical measures.

41      Because the lower crust resides at depths >20 km, its composition can only be sam-  
 42      pled indirectly. Granulite facies lithologies serve as metamorphic analogues for the lower  
 43      crust due to their appearance in exposed crustal cross-sections (Rudnick & Gao, 2003).  
 44      High grade metamorphic terrains, which have been tectonically emplaced in areas such  
 45      as the Ivrea-Verbano Zone in Italy or the Fraser Range in western Australia (Fountain  
 46      & Salisbury, 1981), and granulite facies xenoliths serve as two geochemical windows to  
 47      the lower crust. As a metamorphic facies, characterized by the dehydration of hydrous  
 48      minerals (Semprich & Simon, 2014), granulites span a confounding range of mafic (< 52  
 49      wt. %  $\text{SiO}_2$ ) to felsic (> 68 wt. %  $\text{SiO}_2$ ) compositions. Such wide variation leads to com-  
 50      peting models for the lower crust's composition and density structure, as outlined recently  
 51      by Dumond et al. (2018).

52      Combined modeling of high resolution geophysical and geochemical data can place  
 53      tighter constraints on lower crustal composition. Seismic velocity measurements help dif-  
 54      ferentiate among possible lower crustal compositions when compared to laboratory ex-  
 55      periments (Holbrook et al., 1992). We us seismic inversions in conjunction with petro-  
 56      logical data in an effort to form less biased lower crustal composition model. In this study,  
 57      we target the southwestern United States (Fig. 1) as a demonstration of such joint mod-  
 58      eling efforts because of the variety of data available for the Basin and Range and Col-  
 59      orado Plateau physiographic provinces.

60      Global scale models (Laske et al., 2013; Bassin et al., 2000) predict seismic veloc-  
 61      ities in the Basin and Range that are 10% slower and densities 5% lower than those of  
 62      adjacent tectonic regions. Slower seismic velocities could suggest that the Basin and Range

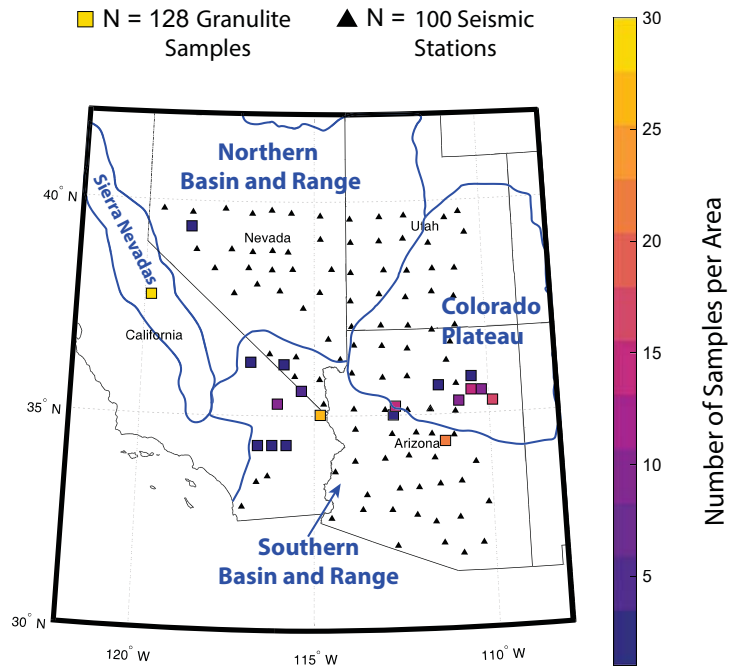


Figure 1: The southwestern United States has been sampled at high resolution through geochemical analyses and ambient noise seismology. The black triangles represent the placement of 100 Earthscope Transportable Array stations whose data were used in this study. Colored squares indicate the location of 128 granulite xenolith and terrain samples used as possible chemical compositions for the lower crust. The color of the squares indicates how many samples were collected from the area covered by the square. The overlaid blue lines demarcate three geologically distinct sub-regions within the study area.

63 has a more felsic lower crust than surrounding areas and stands in contrast to local ve-  
 64 locity studies (Gao & Lekić, 2018; Shen et al., 2013; Olugboji et al., 2017; Plank & Forsyth,  
 65 2016). Both mafic and felsic granulite facies terrains and xenoliths have been extensively  
 66 characterized in the southwestern US, providing us with a geochemical dataset of 128  
 67 samples (<http://www.EarthChem.org/>). We incorporate high resolution, ambient noise,  
 68 dispersion measurements (Olugboji et al., 2017; Ekström, 2014) from the Earthscope US-  
 69 Array (<http://www.usarray.org/>) project; Moho temperature models from Pn veloc-  
 70 ities (Schutt et al., 2018); and thermal gradient calculations to derive a distribution of  
 71 compositions and compositional trends for the lower crust, addressing current model dis-  
 72 crepancies.

## 73 2 Background

### 74 2.1 Compositional Modeling of the Lower Crust

75 The depth and thickness of the lower continental crust varies regionally and in the  
 76 context of different studies. The Conrad discontinuity defines the lower crust seismically  
 77 (Conrad, 1925), but it is not ubiquitous. When the continental crust is split into thirds,  
 78 the average lower crustal composition is typically ~ 53 wt.% SiO<sub>2</sub> (Rudnick & Gao, 2003).  
 79 In some areas, however, the "lower crust" may refer to the bottom half of the continen-  
 80 tal crust, in which case the average SiO<sub>2</sub> becomes more felsic (Hacker et al., 2015). The  
 81 abundance of SiO<sub>2</sub> in the lower crust is not only a function of lower crustal composition,  
 82 but also of one's definition of the lower crust. For the purposes of this study, we define  
 83 the lower crust as simply the bottom half of the crust between 11 km and the Moho (after  
 84 Schmandt et al., 2015). For example, if the Moho depth were 31 km, the lower crust would  
 85 have a thickness of  $\frac{(31-11)}{2} = 10$  km, and range from 21 km - 31 km depth. We des-  
 86 ignate 11 km as the thickness of the upper crust because of changes seen in regional Rayleigh  
 87 wave models from Lin et al. (2014). Though 11 km of upper crust and sediment through-  
 88 out the entire southwestern United States is a sweeping generalization, it is similar to  
 89 Roy et al. (1968) 7-11 km thick heat producing layer and Rudnick and Gao (2003)'s 12  
 90 km thick upper crust. Keep in mind that our compositional trends are more consequen-  
 91 tial than our somewhat arbitrary layer thicknesses.

92 Petrological and geochemical studies of the deep continental crust have sought to  
 93 define composition through analysis of granulite facies xenoliths and terrains where avail-  
 94 able, usually analyzing in detail a small (5 - 20) set of samples. Similar practices have  
 95 been used by many (for example Rudnick & Taylor, 1987; Halliday et al., 1993; Schaaf  
 96 et al., 1994; Parsons et al., 1995; Al-Safarjalani et al., 2009) to determine the deep crustal  
 97 structure in regions where samples are available, but it is hard to gauge if these isolated  
 98 samples are representative of the whole lower crust. While studies of xenoliths provide  
 99 insight into specific areas of the lower crust, limited sample sets and even smaller sam-  
 100 ple sizes prove to be recurring obstacles for geoscientists who seek to uncover the com-  
 101 position of the deep crust as it relates to global processes. Seismological crust models,  
 102 on the other hand, are typically used to describe wide scale crustal phenomena. The use  
 103 of seismic models for determining lower crust composition requires a conversion between  
 104 seismic wave velocities and bulk rock compositions, typically achieved through labora-  
 105 tory experiments (for example, Christensen & Fountain, 1975; Holbrook et al., 1992; Chris-  
 106 tensen & Mooney, 1995). Recent studies (Hacker et al., 2015) give comprehensive assess-  
 107 ments of shear and compressional waves velocities of granulite facies lithologies through  
 108 thermodynamic modeling (calculations are based on empirical, composition-pressure-temperature  
 109 relationships derived from rock mechanics and mineral physics experiments, and ther-  
 110 modynamic theory).

111            **2.2 Geologic Setting**

112            The southwestern United States has undergone multiple episodes of compression  
 113            and extension since the Mesozoic (Coney & Harms, 1984). The elevated Colorado Plateau  
 114            remains relatively undeformed despite being sandwiched between North American Cordillera  
 115            and the Basin and Range. The Basin and Range province, on the other hand, is char-  
 116            acterized by abruptly alternating basins and narrow mountain chains that arose from  
 117            tensional stress and normal faulting in the Early Miocene (17 Ma) (Coney, 1980). The  
 118            Basin and Range extended crust, in conjunction with the Colorado Plateau, houses Ceno-  
 119            zoic volcanics that are thought to be linked to changes in plate interactions after the con-  
 120            clusion of the Laramide Orogeny (McKee, 1971). The deep crustal xenoliths delivered  
 121            through Cenozoic volcanic eruptions provide one of our sources of geochemical data. A  
 122            second data source are the Basin and Range's metamorphic core complexes - a belt of  
 123            medium- to high-grade metamorphic terrains exhumed through crustal extension (Crittenden  
 124            et al., 1980). A suite of crust deformation models have been proposed to produce these  
 125            core complexes (Cooper et al., 2010), each model a different combination of brittle fault-  
 126            ing and ductile extension.

127            **3 Methods**

128            We used a three-step joint geochemical-geophysical modeling process to constrain  
 129            composition. Figure 2 provides a schematic walk-through of the inputs and outputs of  
 130            each step.

131            First, we calculated physical properties over a range of pressures and temperatures  
 132            for local granulite facies samples through the thermodynamic Gibbs free energy mini-  
 133            mization software Perple\_X (Connolly, 2005). Second, we determined pressure-temperature  
 134            conditions at 1 km intervals within the lower crust, making the assumption that pres-  
 135            sure uniformly increases 1 GPa per 35 km depth, or roughly 28.6 MPa (286 bars) per  
 136            kilometer. Temperature inputs at the top and base of the crust allowed us to calculate  
 137            a geothermal gradient and therefore a temperature for each kilometer within the crust,  
 138            assuming that the top of the crust resides at  $5 \pm 5^{\circ}\text{C}$  and temperature at the Moho fol-  
 139            lows Schutt et al. (2018). Third, we compared the Perple\_X-calculated shear wave ve-  
 140            locities ( $\text{Vs}$ ) of each sample to seismic inversions for  $\text{Vs}$ . We calculated the probability  
 141            of each sample producing the observed seismic signal by convolving the two datasets.

142            In general, we favored the simplest parameter space that could explain the geochem-  
 143            ical observations in our dataset. A full explanation of the Perple\_X parameters we used  
 144            and our rationale is given in the Supplement. Olugboji et al. (2017) and Ekström (2014)  
 145            explain the inversion techniques that produced our seismic profiles.

146            We evaluated the uncertainties associated with each step of our combined model,  
 147            allowing for variations in lower crustal thickness, temperature, and seismic velocity (Ta-  
 148            ble 1). Moho depths were assigned a 2 km uncertainty (Shen & Ritzwoller, 2016), and  
 149            Moho temperature uncertainties range from 50 to  $80^{\circ}\text{C}$  depending on location (Schutt  
 150            et al., 2018). Combined variations in Moho temperature and depth, and a linear extrap-  
 151            olation of temperature through the crust (Blackwell, 1971) gave us variable temperature  
 152            gradients throughout the area of study, which we calculated via Monte Carlo simulation.  
 153            The result is a distribution of possible lower crustal pressure-temperature conditions, which  
 154            translated to a probability distribution of compositions. Convolving the distribution of  
 155            Perple\_X generated velocities with the seismic shear wave velocities produced our final  
 156            distribution.

157            Systematic uncertainties may exist if our fundamental assumption of a dry, gran-  
 158            ulte facies lower crust is inaccurate. The accuracy of Perple\_X's velocity calculations  
 159            depends largely on this assumption, as a lack of water restricts our compositions to an-

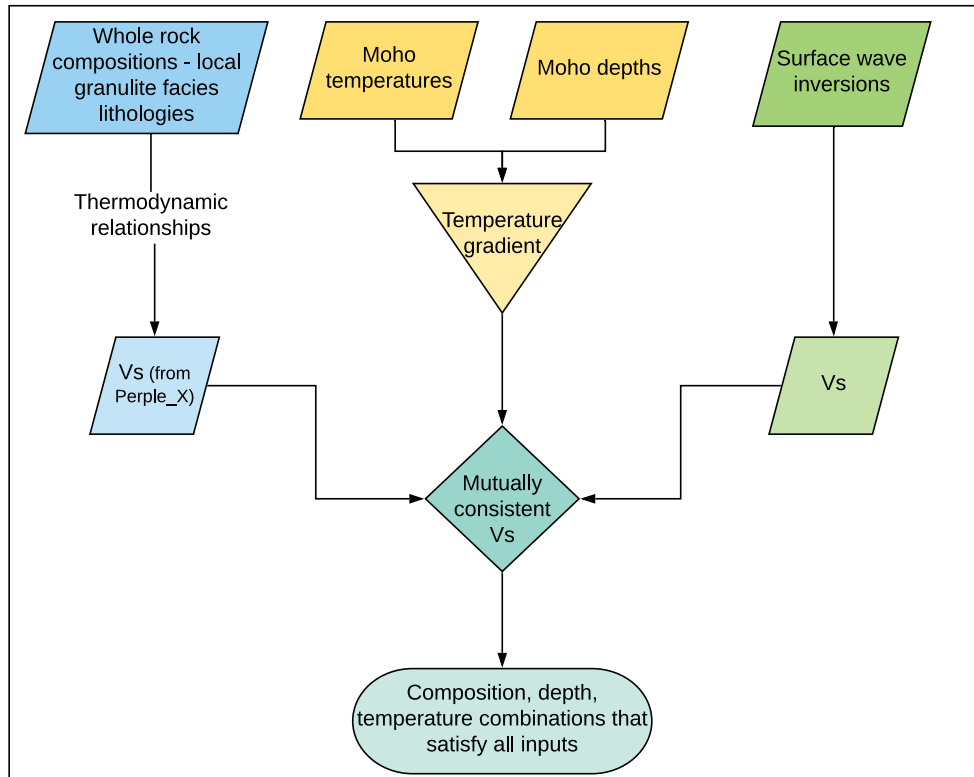


Figure 2: Crust modeling flowchart showing our procedure for finding consistent models based on Vs, temperature, depth, and composition. Seismic velocity map from Olugboji et al. (2017); Moho temperatures based on Schutt et al. (2018); Moho depths from CRUST1.0 (Laske et al., 2013).

Table 1: Uncertainties Associated with Methods

Parameter	Uncertainty
Seismic velocity inversions	full distribution compared to geochemical results, uncertainties on seismic inversion methods given from Gao and Lekić (2018)
Perple_X calculations	< 1% uncertainty from calculations, but subject to unknown systematic uncertainty
Moho temperature	5%-10% (Schutt et al., 2018)
Lower crustal thickness	13% - 25%, assuming absolute uncertainty of 2 km (Buehler & Shearer, 2017)

160 hydrous minerals. Connolly (2005) offers an overview of the software's free energy minimization technique for calculating mineral assemblages.  
 161

## 162 4 Results

163 Overall, the hot lower crust of the southwestern United States trends towards intermediate and mafic compositions. When investigating sub-regional scale variations, how-  
 164 ever, three separate trends of composition emerge. Joint modeling of surface wave ve-  
 165 locities and geochemical and petrological data yields a variety of compositions that de-  
 166 pend on temperature. An iterative approach allows us to construct a distribution of prob-  
 167 able compositions at each of 100 seismic stations, to account for uncertainties in tem-  
 168 perature and composition. Any granulite compositions that were duplicates (i.e. sam-  
 169 ples whose Vs's or compositions were indistinguishable from another sample's) were re-  
 170 moved to avoid artificially weighting our results towards redundantly-sampled litholo-  
 171 gies.  
 172

173 Similar velocities and compositions are evident among three sub-provinces of the  
 174 study area: the Colorado Plateau to the east, the beginnings of the Northern Basin and  
 175 Range in the northwest, and the Southern Basin and Range in the southwest. As a whole,  
 176 the shear wave velocities of all three regions range from 3.8 km/s to 4.2 km/s, with about  
 177 half of the lower crust being faster than 4.0 km/s (Fig. 3). Vp, calculated from Perple\_X,  
 178 often exceeds 7.0 km/s in the Southern Basin and Range and in deeper portions of the  
 179 Northern Basin and Range and Colorado Plateau. The Southern Basin and Range, which  
 180 has experienced the most recent tectonic activity, is marked by the thinnest, hottest crust,  
 181 while the Colorado Plateau has the thickest, coolest crust. Despite comparatively slow  
 182 Vs in the Southern Basin and Range ( $3.9 \pm 0.1$  km/s), its high temperatures (often  $>$   
 183  $800^\circ\text{C}$ ) require a Vp of  $7.1 \pm 0.1$  km/s and a density of  $3000 \pm 190 \text{ kg/m}^3$  at the base  
 184 of the crust to satisfy the geophysical model (Fig. 3). The Vp/Vs ratio remains poorly  
 185 constrained, with uncertainties upwards of 10% encompassing most lithologies (Brocher,  
 186 2005). Figure 3 illustrates a change in the median Vp/Vs from  $\sim 1.79$  to  $\sim 1.72$  sep-  
 187 arating the Colorado Plateau from the Basin and Range, a shift that reflects composi-  
 188 tional variation.

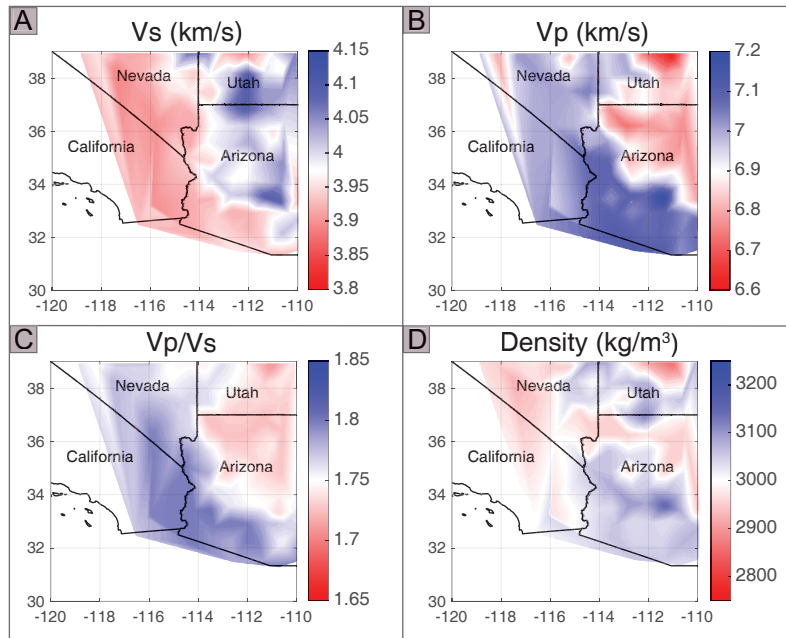


Figure 3: Joint geophysical-geochemical predicted median Vs, Vp, Vp/Vs, and density (3A - 3D, respectively) over all depths for the southwestern United States. The Colorado Plateau is clearly differentiated from the Basin and Range in Vp and Vp/Vs. Hotter temperatures in the south lead to slower Vs but faster Vp and higher densities in the Southern Basin and Range. Blue regions in B, C, and D correspond to more mafic compositions.

Not surprisingly, compositional trends follow velocity trends, forming three distinct compositional provinces. Figure 4 shows representative distributions of  $\text{SiO}_2$  content that result from our inversions. The Colorado Plateau, which has the coolest crust and the lowest Vp/Vs ratio, also has the widest distribution of possible compositions (Fig. 4A), which range from 45 to roughly 75 wt.%  $\text{SiO}_2$ . The Basin and Range favors narrower, more mafic distributions (Fig. 4B and C). Regardless of location, though, mafic lithologies can explain the lower crust's seismic profile more frequently with increasing depth, as shown by the increasing blueness with depth of Figure 4. Figure 5 (and Figure S3) maps reveal clear compositional distinctions among the three sub-provinces. The differences between the intermediate  $\text{SiO}_2$  Colorado Plateau, intermediate-mafic Northern Basin and Range, and mafic Southern Basin and Range are most apparent in the shallow lower crust. Both the Colorado Plateau and the Northern Basin and Range increase in MgO and FeO content and decrease in  $\text{SiO}_2$  content at greater depths, but the Colorado Plateau does not reach truly mafic compositions until 35 - 40 km depth.

Six mineral groups dominate the modeled lower crustal mineralogy. Clinopyroxene and garnet grow at the expense of quartz and plagioclase and K-feldspars in deeper portions of the crust. Orthopyroxene abundances also decrease by a few weight % with depth. The high abundance ( $\sim 3.5 - 16$  wt.%) of K-feldspars (which primarily manifests sanidine under simulated pressure and temperature conditions) reflects the alkali-rich, latite-like compositions of crystalline rocks from the southwestern United States (Tyner & Smith, 1986). At shallower pressures and colder temperatures, minerals such as kyanite, sillimanite, or ilmenite can comprise anywhere from 5 - 15 wt.% of the "lower crust".

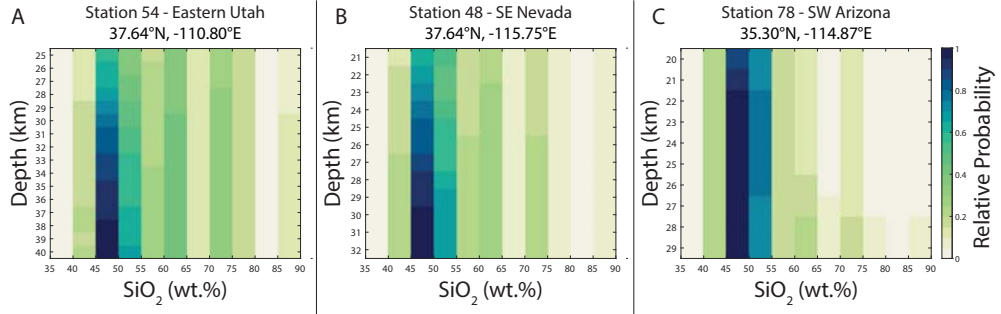


Figure 4: Representative histograms (A-C) of the three "sub-provinces" within the study area show increasing probability of a mafic crust with increasing depth. Color indicates the relative probability of a given  $\text{SiO}_2$  abundance explaining the seismic signal at a given depth. The thicker, cooler Colorado Plateau (A) can, on average, accommodate a higher percentage of  $\text{SiO}_2$  than the Northern (B) or Southern (C) Basin and Range.

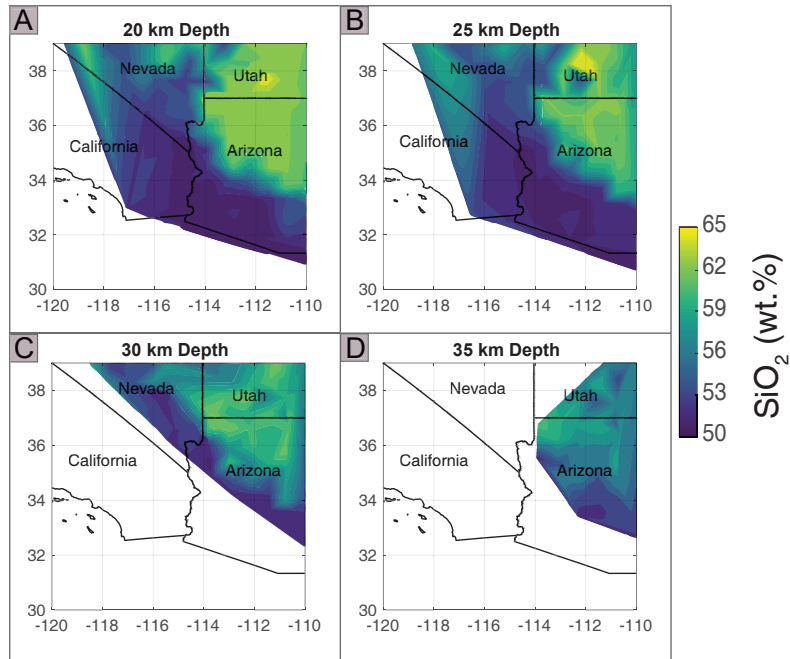


Figure 5: Variability in median  $\text{SiO}_2$  abundance in the southwestern United States tracks the Colorado Plateau (high  $\text{SiO}_2$ ), Northern Basin and Range (medium  $\text{SiO}_2$ ), and Southern Basin and Range (low  $\text{SiO}_2$ ).  $\text{SiO}_2$  abundance overall decreases with increasing depth (A - D). Color scale indicates wt.%  $\text{SiO}_2$ . Mantle compositions are not shown in this figure, and therefore deeper profiles (e.g. C - D) show only regions with greater crustal thickness.

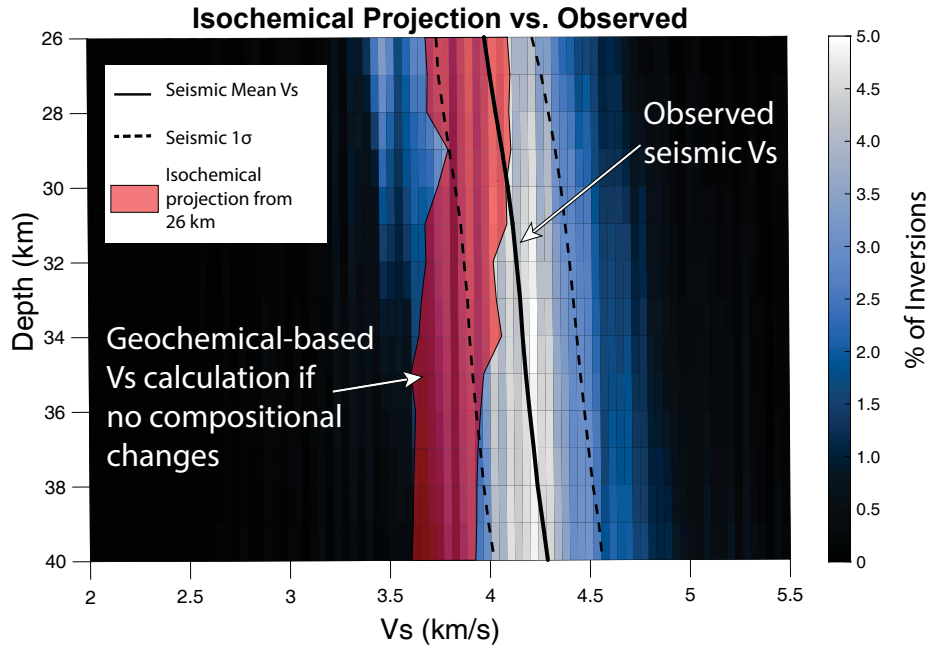


Figure 6: An example of granulite lithologies fitting the seismic signal at the top of the lower crust projected to higher temperature and pressure conditions (red field). This isochemical predicted Vs projection deviates substantially from the mean seismic Vs to the extent that by 38 km depth the distributions are distinguishable at  $1\sigma$ . (For comparison, seismic Vs is typically reported as mean  $\pm 1$  standard error of the mean. Using this metric, the distributions become distinguishable at 30 km.)

211 Mineral assemblages simplify at greater depths, with clinopyroxene, garnet, plagioclase,  
212 and quartz often controlling >80% of the mineralogy.

213 Though it is convenient to report one number and an uncertainty as representative  
214 for composition, we must be mindful that the shapes of these major oxide and min-  
215 eral distributions are non-normal and cannot be fully described by simple summary statis-  
216 tics. That being said, whether reporting mean or median value as representative of the  
217 lower crust, the trend of vertical change in composition holds true for the Colorado Plateau  
218 and Northern Basin and Range (see Tables 2 - 3). The Southern Basin and Range mean  
219 composition shows this gradient to a lesser extent, while the median is homogeneously  
220 mafic. For the sake of convenience, our interpretations will reference the median  $\pm \frac{1}{2}$  the  
221 inter-quartile range (IQR) compositions unless stated otherwise. We favor the median  
222 and IQR because they are more resistant to outliers than the mean.

## 223 5 Discussion

### 224 5.1 Lower Crust Composition

225 One value, one composition, is insufficient for describing the entirety of the con-  
226 tinental lower crust. We can describe the lower crust more accurately by reporting changes  
227 in velocity, density, and composition as a function of depth and location. The lower con-  
228 tinental crust, though less than 8 km thick in some sections of the southwestern United  
229 States (Buehler & Shearer, 2017), undoubtedly displays lateral and vertical heterogene-

Table 2: Colorado Plateau SiO<sub>2</sub> Content

Depth	Mean	Median	Standard Deviation	1st Quartile	3rd Quartile
26	60.0	58.8	11.6	50.0	69.7
27	59.8	58.6	11.8	49.5	69.9
28	59.6	58.3	11.7	49.5	69.5
29	59.3	57.8	11.7	49.3	69.2
30	59.0	57.4	11.7	49.1	68.7
31	58.8	56.8	11.8	48.8	68.6
32	58.6	56.2	11.8	48.6	68.1
33	58.3	55.8	11.8	48.5	67.3
34	58.1	55.2	11.7	48.4	66.8
35	57.9	54.7	11.7	48.3	66.4
36	57.7	54.3	11.7	48.3	65.9
37	57.5	53.7	11.6	48.2	65.3
38	57.3	53.4	11.6	48.1	64.8
39	57.1	53.1	11.5	48.1	64.4
40	56.9	52.8	11.5	48.0	64.0

Oxide abundances reported in wt.%.

Table 3: Northern Basin and Range SiO<sub>2</sub> Content

Depth	Mean	Median	Standard Deviation	1st Quartile	3rd Quartile
22	58.3	55.1	10.8	49.9	65.7
23	58.3	55.1	10.9	50.0	65.4
24	58.1	54.7	10.9	49.7	65.0
25	58.0	54.4	11.0	49.7	64.9
26	57.7	54.0	10.9	49.5	64.3
27	57.7	53.9	11.1	49.2	64.2
28	57.4	53.6	11.0	49.1	63.8
29	57.4	53.6	11.1	48.9	64.0
30	57.2	53.4	11.2	48.8	63.6
31	57.0	52.9	11.2	48.6	63.4
32	57.0	52.8	11.4	48.3	63.7

Oxide abundances reported in wt.%.

Table 4: Southern Basin and Range SiO<sub>2</sub> Content

Depth	Mean	Median	Standard Deviation	1st Quartile	3rd Quartile
19	54.6	51.2	10.0	48.0	58.1
20	54.3	51.1	9.9	48.0	57.6
21	54.1	51.1	9.8	47.9	57.0
22	54.0	51.2	9.7	47.9	56.8
23	54.0	51.2	9.7	48.0	56.6
24	53.9	51.1	9.6	47.9	56.3
25	53.9	51.2	9.6	47.8	56.4
26	53.8	51.3	9.6	47.9	56.2
27	54.0	51.4	9.7	47.9	56.7

Oxide abundances reported in wt.%.

Table 5: South Western United States Lower Crust Major Oxide Content

	Mean	Median	Standard Deviation	1st Quartile	3rd Quartile
SiO <sub>2</sub>	56.9	53.7	10.6	49.1	63.5
Al <sub>2</sub> O <sub>3</sub>	16.7	16.1	4.3	14.1	19.5
MgO	5.4	3.8	4.2	2.5	7.3
FeO	8.6	7.7	4.1	5.5	11.4
CaO	7.0	5.6	4.9	2.2	10.6
K <sub>2</sub> O	1.6	1.3	1.5	0.4	2.2
Na <sub>2</sub> O	2.7	2.7	1.4	1.6	3.8
TiO <sub>2</sub>	1.1	0.9	0.8	0.5	1.4

Overall lower crust oxide abundances for the southwestern United States.

Table 6: Summary of Lower Crust Seismic Properties and Mineralogy

	Mean	Median	Standard Deviation	1st Quartile	3rd Quartile
Vs*	3.62	3.61	0.36	3.30	3.64
Vs**	4.02	3.99	0.23	3.86	4.15
Vp	6.94	6.91	0.44	6.59	7.27
Vp/Vs	1.73	1.75	0.07	1.68	1.78
Density	3010	3000	220	2820	3190
Clinopyroxene	17.5	13.3	16.6	3.4	31.5
Garnet	13.0	11.8	8.7	6.5	18.1
K-feldspars	10.9	8.2	6.7	3.4	16.0
Kyanite	3.5	2.5	4.1	0.5	5.3
Olivine	1.3	0.03	5.8	0	0.3
Orthopyroxene	3.0	1.5	4.3	0.2	5.0
Plagioclase	30.3	27.6	14.0	15.5	43.5
Quartz	12.7	10.9	16.1	0.7	27.0

\*Vs from surface wave inversions

\*\*Vs from combined surface wave and geochemical model

ity (Fig. 5 and S3). Temperature plays a crucial role in determining lower crustal composition. Both cold intermediate and hot mafic granulites can produce the shear wave velocities of >3.9 km/s observed across the southwestern United States (Christensen & Mooney, 1995). The thicker, cooler crust of the Colorado Plateau (average Moho temperature 700°C, constant gradient of 17.5°C/km) and Northern Basin and Range (average Moho temperature 740°C, constant gradient of 22.4°C/km) can therefore accommodate  $55.8 \pm 9.4$  and  $53.9 \pm 7.5\%$  SiO<sub>2</sub>, respectively. The Southern Basin and Range, in contrast, must have a predominantly mafic composition of  $51.2 \pm 4.3\%$  SiO<sub>2</sub> to reach similar Vs because of its thin crust and 800°C temperatures.

The temperature gradient in the lower crust also necessitates a vertical gradient in mineralogy and composition. The crust becomes increasingly mafic with increasing depth. This trend is observed most prominently in areas of thicker crust. The increase in Vs cannot be explained by isochemical chemical changes in the lower crust - that is, we cannot explain the observed Vs by simply projecting mid-crustal compositions to higher pressures and temperatures (Figure 6). As noted by Christensen and Mooney (1995), we must invoke a compositional gradient within the lower crust to explain the increase in seismic velocity.

In the topmost portions of the Colorado Plateau's lower crust, our model can accommodate over 59 wt.% SiO<sub>2</sub> (Table 2). However, such intermediate-felsic material cannot reach high enough velocities to match the seismic signal deeper in the crust, where temperatures increase above 700°C (Schutt et al., 2018). Furthermore, our set of granulites can explain the seismic signal at the base of the crust more often than at the top, whereas we might expect equal probabilities at all depths if the lower crust were compositionally uniform (shown by the colors of Fig. 4). The Northern Basin and Range and Colorado Plateau (Fig. 5) show 3 – 6 wt.% decrease in SiO<sub>2</sub> and an increase in MgO, FeO, and CaO with increasing depth. The Southern Basin and Range, though, seems to lack this trend, the lower crust remaining consistently at 51 wt.% SiO<sub>2</sub>. This is pos-

257 sibly due to removal of more felsic material from the top of the crustal column, which  
 258 we discuss in section 5.1.1.

259 The specific mineralogy of the lower crust is trickier to constrain than the bulk com-  
 260 position because of its strong dependence on our initial assumptions. Provided that our  
 261 lower crust is dry and equilibrated in the granulite metamorphic facies, we expect to see  
 262 mineral assemblages that are rich in clinopyroxenes, garnets, and plagioclase feldspars  
 263 (Rudnick & Fountain, 1995). Few studies that characterize the whole rock compositions  
 264 of granulite quantitatively report mineralogy. This makes comparison between our re-  
 265 sults and petrological studies of our samples difficult. Though Perple\_X builds bulk rock  
 266 velocities from mineral constituents, many mafic rock forming minerals have similar Vs  
 267 under lower crustal pressure and temperature conditions (e.g. at 650°C and 0.85 GPa  
 268 diopside: 4.60 km/s; almandine: 4.57 km/s; spessartine: 4.65 km/s; anorthite: 3.65 km/s;  
 269 sanidine: 3.49 km/s). A sample may therefore change mineralogy without drastically chang-  
 270 ing its bulk rock properties or composition. In addition, our model's mineralogy predic-  
 271 tions are more sensitive to temperature than its seismic velocity predictions are, due to  
 272 the abrupt and complete phase changes implemented by Perple\_X. We do not have the  
 273 seismic resolution to see such sharp changes in reality (Olugboji et al., 2017), if they ex-  
 274 ist at all.

275 However, retrograde metamorphism is unlikely to occur due to the thermodynamic  
 276 barrier of rehydration (Semprich & Simon, 2014), and the base of the lower crust must  
 277 be mafic in our model no matter *which* mafic minerals specifically are present. Broadly  
 278 speaking, the abundance of garnet and clinopyroxene increases with depth, driving the  
 279 increase in Vs. Mineral assemblages simplify with increasing depth and temperature, leav-  
 280 ing little room for accessory phases, such as ilmenite and kyanite, at the base of the crust.

281 Further seismic constraints could reduce the uncertainty on our compositions. The  
 282 Vp/Vs ratio can often distinguish mafic from felsic compositions (Holbrook et al., 1992).  
 283 A Vp/Vs of  $>1.65$  would reduce the probability of lower crustal compositions  $>65$  wt.%  
 284 SiO<sub>2</sub> (Holbrook et al., 1992) (or, conversely, Vp/Vs of  $<1.65$  would indicate that geo-  
 285 chemical studies over-sample mafic compositions). Given that most crystalline rocks ex-  
 286 hibit Vp/Vs between 1.6 - 1.9 at standard experiment conditions (Brocher, 2005), the  
 287 ratio would have to be tightly constrained at  $<\pm 7\%$  variation. Future quantitatively  
 288 robust modeling efforts of the southwestern United States should also investigate the pres-  
 289 ence of hydrous minerals (Valentine & Perry, 2007; Dixon et al., 2004) and melt (Rey  
 290 et al., 2009) in the lower crust. The presence of fluids could lower the deep crust's Vs,  
 291 requiring compositions that are even more mafic than those reported here. Alternatively,  
 292 melt could cause the temperatures implemented in this study to be over-predicted (Schutt  
 293 et al., 2018).

### 294 5.1.1 Implications for Crust Formation

295 Ductile spreading and uplift of the lower crust could explain the correlation between  
 296 crustal thickness and composition. Brittle thinning of the upper and/or middle crust through  
 297 normal faulting allows for isostatic uplift of ductile, deeper crust with little change in  
 298 lower crustal thickness (Cooper et al., 2010), illustrated by Figure 7. Because the thinnest  
 299 regions of the southwestern United States are also the most mafic, what was once "lower  
 300 crust" now likely comprises a greater volume of the 25-28 km thick crustal column. Crustal  
 301 thickness was lost as intermediate and felsic material was removed from the top, rather  
 302 than through lower crustal delamination (Rudnick & Gao, 2003). The composition of  
 303 the deepest layers of Northern Basin and Range are similar to the deep Colorado Plateau  
 304 53 wt.% SiO<sub>2</sub>, further suggesting that the extended crust has not lost a mafic root rel-  
 305 ative to the thicker crust. Had crustal thinning been caused by delamination, the thinnest  
 306 Southern Basin and Range crust would be the most felsic rather than the most mafic.  
 307 Based on the lower crust's mafic composition, the eclogitization process required for de-

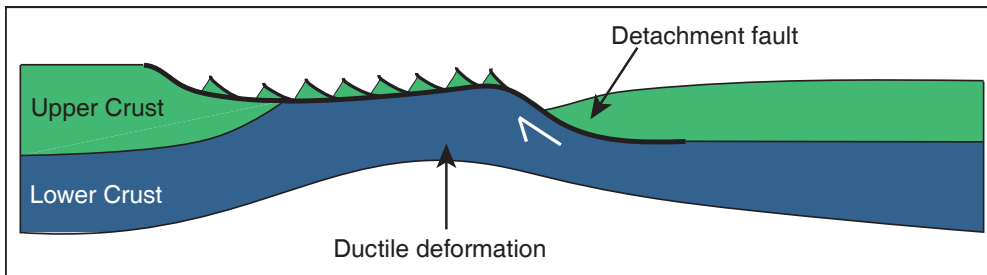


Figure 7: The west-east schematic cross-section of the southwestern United States deformation that our model supports. Crustal extension is accommodated primarily through brittle faulting in the upper crust, which is separated from the lower crust by a rolling hinge detachment Cooper et al. (2010). The ductilely deformed lower crust is uplifted but not substantially thinned.

308 lamination would likely only be triggered at high pressures (Semprich & Simon, 2014).  
 309 While the Basin and Range is certainly hot enough to undergo delamination (Jull & Kele-  
 310 men, 2001), it would have had to occur during a time of crustal thickening (for instance,  
 311 during the Laramide Orogeny (Bird, 1984; Livaccari, 1991), not during extension.

## 312 6 Conclusion

313 Joint modeling of geophysical and geochemical properties of the lower crust can  
 314 help constrain lower crustal composition. As an example, in the southwestern United States,  
 315 seismic velocities, when paired with Moho temperatures and thermodynamic calculations,  
 316 indicates that the lower crust transitions from intermediate to mafic composition,  $\text{SiO}_2$   
 317 content decreasing by up to 6% with increasing depth. Temperature gradients cause com-  
 318 positional distinctions to arise among the relatively cool Colorado Plateau, the warm North-  
 319 ern Basin and Range, and the hot Southern Basin and Range. The predominantly mafic  
 320 composition of the lower crust reflects the tectonic history of this region and can help  
 321 distinguish between different crust deformation mechanisms.

322 Though global-scale models give a generalized view of the lower crust, nonunique  
 323 solutions to composition can be better constrained in regional-scale studies by combin-  
 324 ing high resolution local datasets and compositional proxies. Combining seismological,  
 325 petrological, and thermodynamic data opens avenues for future detailed investigation  
 326 into deep crust composition and structure.

## 327 7 Author Contributions

328 L.G.S. wrote this text and modeled the lower crustal compositions with help from  
 329 C.G. C.G. provided ambient noise inversions. W.F.M. contributed significantly to data  
 330 analysis and text. The authors would also like to thank the University of Maryland - Uni-  
 331 versity of California, Santa Barbara joint crust discussion group for fruitful insights on  
 332 model development and interpretation of results. All authors have read and approved  
 333 this manuscript.

## 334 Acknowledgments

335 W.F.M. would like to acknowledge the NSF for support (grant EAR1650365). Model re-  
 336 sults and original code are provided at DOI 10.5281/zenodo.3530768. Geochemical data  
 337 were provided by Earthchem.org (<http://www.EarthChem.org/>). Seismic data provided

338 by the Earthscope USArray project (<http://www.usarray.org/>). There are no financial  
 339 or interest conflicts with this work.

340 **References**

- 341 Al-Safarjalani, A., Nasir, S., Fockenberg, T., & Massonne, H.-J. (2009). Chemical  
 342 composition of crustal xenoliths from southwestern Syria: Characterization of  
 343 the upper part of the lower crust beneath the Arabian plate. *Geochemistry*,  
 344 69(4), 359-375. doi: 10.1016/j.chemer.2009.05.005
- 345 Bassin, C., Laske, G., & Masters, G. (2000). The current limits of resolution for sur-  
 346 face wave tomography in {North America}. *Eos*, 81.
- 347 Bird, P. (1984). Laramide crustal thickening event in the Rocky Mountain Foreland  
 348 and Great Plains. *Tectonics*, 3(7), 741-758. doi: 10.1029/TC003i007p00741
- 349 Blackwell, D. D. (1971). Heat flow. *Eos, Transactions American Geophysical Union*,  
 350 52(5), IUGG 135. doi: 10.1029/EO052i005pIU135
- 351 Brocher, T. M. (2005). Empirical Relations between Elastic Wavespeeds and Density  
 352 in the Earth's Crust. *Bulletin of the Seismological Society of America*, 95(6),  
 353 2081-2092. doi: 10.1785/0120050077
- 354 Buehler, J., & Shearer, P. (2017). Uppermost mantle seismic velocity structure be-  
 355 neath usarray. *Journal of Geophysical Research: Solid Earth*, 122(1), 436-448.
- 356 Christensen, N. I., & Fountain, D. M. (1975). Constitution of the Lower Continental  
 357 Crust Based on Experimental Studies of Seismic Velocities in Granulite. *Geo-  
 358 logical Society of America Bulletin*, 86(2), 227. doi: 10.1130/0016-7606(1975)  
 359 86<227:COTLCC>2.0.CO;2
- 360 Christensen, N. I., & Mooney, W. D. (1995). Seismic velocity structure and compo-  
 361 sition of the continental crust: A global view. *Journal of Geophysical Research:  
 362 Solid Earth*, 100(B6), 9761-9788. doi: 10.1029/95JB00259
- 363 Coney, P. J. (1980). Cordilleran metamorphic core complexes: An overview.  
 364 *Cordilleran metamorphic core complexes: Geological Society of America Mem-  
 365 oir*, 153, 7-31.
- 366 Coney, P. J., & Harms, T. A. (1984). Cordilleran metamorphic core complexes:  
 367 Cenozoic extensional relics of mesozoic compression. *Geology*, 12(9), 550-554.
- 368 Connolly, J. A. D. (2005). Computation of phase equilibria by linear program-  
 369 ming: A tool for geodynamic modeling and its application to subduction zone  
 370 decarbonation. *Earth and Planetary Science Letters*, 236(1), 524-541. doi:  
 371 10.1016/j.epsl.2005.04.033
- 372 Conrad, V. (1925). *Laufzeitkurven des tauernbebens vom 28. nov. 1923*.
- 373 Cooper, F. J., Platt, J. P., Anczkiewicz, R., & Whitehouse, M. J. (2010). Footwall  
 374 dip of a core complex detachment fault: Thermobarometric constraints from  
 375 the northern Snake Range (Basin and Range, USA). *Journal of Metamorphic  
 376 Geology*, 28(9), 997-1020. doi: 10.1111/j.1525-1314.2010.00907.x
- 377 Crittenden, M. D., Coney, P. J., Davis, G. H., & Davis, G. H. (1980). *Cordilleran  
 378 metamorphic core complexes* (Vol. 153). Geological Society of America.
- 379 Dixon, J. E., Dixon, T. H., Bell, D. R., & Malservisi, R. (2004). Lateral variation  
 380 in upper mantle viscosity: Role of water. *Earth and Planetary Science Letters*,  
 381 222(2), 451-467. doi: 10.1016/j.epsl.2004.03.022
- 382 Dumond, G., Williams, M. L., & Regan, S. P. (2018). The athabasca granulite ter-  
 383 rane and evidence for dynamic behavior of lower continental crust. *Annual Re-  
 384 view of Earth and Planetary Sciences*, 46, 353-386.
- 385 Ekström, G. (2014). Love and rayleigh phase-velocity maps, 5–40 s, of the western  
 386 and central usa from usarray data. *Earth and Planetary Science Letters*, 402,  
 387 42-49.
- 388 Fountain, D. M., & Salisbury, M. H. (1981). Exposed cross-sections through the  
 389 continental crust: implications for crustal structure, petrology, and evolution.  
 390 *Earth and Planetary Science Letters*, 56, 263-277.

- 391 Gao, C., & Lekić, V. (2018). Consequences of parametrization choices in surface  
 392 wave inversion: Insights from transdimensional Bayesian methods. *Geophysical*  
 393 *Journal International*, 215(2), 1037-1063. doi: 10.1093/gji/ggy310
- 394 Hacker, B. R., Kelemen, P. B., & Behn, M. D. (2015). Continental Lower Crust.  
 395 *Annual Review of Earth and Planetary Sciences*, 43(1), 167-205. doi: 10.1146/  
 396 annurev-earth-050212-124117
- 397 Halliday, A. N., Dickin, A. P., Hunter, R. N., Davies, G. R., Dempster, T. J., Hamil-  
 398 ton, P. J., & Upton, B. G. J. (1993). Formation and composition of the lower  
 399 continental crust: Evidence from Scottish xenolith suites. *Journal of Geophys-  
 400 ical Research: Solid Earth*, 98(B1), 581-607. doi: 10.1029/92JB02276
- 401 Holbrook, W. S., Mooney, W. D., & Christensen, N. I. (1992). The seismic velocity  
 402 structure of the deep continental crust. *Continental lower crust*, 23, 1-43.
- 403 Jackson, J. (2002). Strength of the continental lithosphere: time to abandon the  
 404 jelly sandwich? *GSA today*, 12, 4-10.
- 405 Jull, M., & Kelemen, P. B. (2001). On the conditions for lower crustal convective  
 406 instability. *Journal of Geophysical Research: Solid Earth*, 106(B4), 6423-6446.  
 407 doi: 10.1029/2000JB900357
- 408 Laske, G., Masters, G., Ma, Z., & Pasyanos, M. (2013). Update on crust1. 0—a 1-  
 409 degree global model of earth's crust. In *Geophys. res. abstr* (Vol. 15, p. 2658).
- 410 Lin, F.-C., Tsai, V. C., & Schmandt, B. (2014). 3-d crustal structure of the west-  
 411 ern united states: application of rayleigh-wave ellipticity extracted from noise  
 412 cross-correlations. *Geophysical Journal International*, 198(2), 656-670.
- 413 Livaccari, R. F. (1991). Role of crustal thickening and extensional collapse in the  
 414 tectonic evolution of the Sevier-Laramide orogeny, western United States. *Ge-  
 415 ology*, 19(11), 1104-1107. doi: 10.1130/0091-7613(1991)019<1104:ROCTAE>2.3  
 416 .CO;2
- 417 McKee, E. (1971). Tertiary igneous chronology of the great basin of western united  
 418 states—implications for tectonic models. *Geological Society of America Bulletin*,  
 419 82(12), 3497-3502.
- 420 Olugboji, T., Lekic, V., & McDonough, W. (2017). A statistical assessment of  
 421 seismic models of the us continental crust using bayesian inversion of ambient  
 422 noise surface wave dispersion data. *Tectonics*, 36(7), 1232-1253.
- 423 Parsons, T., Christensen, N. I., & Wilshire, H. G. (1995). Velocities of south-  
 424 ern Basin and Range xenoliths: Insights on the nature of lower crustal  
 425 reflectivity and composition. *Geology*, 23(2), 129-132. doi: 10.1130/  
 426 0091-7613(1995)023<0129:VOSBAR>2.3.CO;2
- 427 Plank, T., & Forsyth, D. W. (2016). Thermal structure and melting conditions in  
 428 the mantle beneath the basin and range province from seismology and petrol-  
 429 ogy. *Geochemistry, Geophysics, Geosystems*, 17(4), 1312-1338.
- 430 Rey, P. F., Teyssier, C., & Whitney, D. L. (2009). Extension rates, crustal melting,  
 431 and core complex dynamics. *Geology*, 37(5), 391-394. doi: 10.1130/G25460A  
 432 .1
- 433 Roy, R. F., Blackwell, D. D., & Birch, F. (1968). Heat generation of plutonic rocks  
 434 and continental heat flow provinces. *Earth and Planetary Science Letters*, 5,  
 435 1-12.
- 436 Rudnick, R. L., & Fountain, D. M. (1995). Nature and composition of the continen-  
 437 tal crust: A lower crustal perspective. *Reviews of Geophysics*, 33(3), 267-309.  
 438 doi: 10.1029/95RG01302
- 439 Rudnick, R. L., & Gao, S. (2003). Composition of the continental crust. *Treatise on  
 440 geochemistry*, 3, 659.
- 441 Rudnick, R. L., & Taylor, S. R. (1987). The composition and petrogenesis of the  
 442 lower crust: A xenolith study. *Journal of Geophysical Research: Solid Earth*,  
 443 92(B13), 13981-14005. doi: 10.1029/JB092iB13p13981
- 444 Schaaf, P., Heinrich, W., & Besch, T. (1994). Composition and Sm-Nd isotopic  
 445 data of the lower crust beneath San Luis Potosí, central Mexico: Evidence

- 446 from a granulite-facies xenolith suite. *Chemical Geology*, 118(1), 63-84. doi:  
447 10.1016/0009-2541(94)90170-8
- 448 Schmandt, B., Lin, F.-C., & Karlstrom, K. E. (2015). Distinct crustal isostasy  
449 trends east and west of the rocky mountain front. *Geophysical Research Letters*,  
450 42(23), 10-290.
- 451 Schutt, D. L., Lowry, A. R., & Buehler, J. S. (2018). Moho temperature and mobil-  
452 ity of lower crust in the western United States. *Geology*, 46(3), 219-222. doi:  
453 10.1130/G39507.1
- 454 Semprich, J., & Simon, N. S. C. (2014). Inhibited eclogitization and consequences  
455 for geophysical rock properties and delamination models: Constraints from  
456 cratonic lower crustal xenoliths. *Gondwana Research*, 25(2), 668-684. doi:  
457 10.1016/j.gr.2012.08.018
- 458 Shen, W., & Ritzwoller, M. H. (2016). Crustal and uppermost mantle structure  
459 beneath the United States. *Journal of Geophysical Research: Solid Earth*,  
460 121(6), 4306-4342. doi: 10.1002/2016JB012887
- 461 Shen, W., Ritzwoller, M. H., & Schulte-Pelkum, V. (2013). A 3-D model of the crust  
462 and uppermost mantle beneath the Central and Western US by joint inver-  
463 sion of receiver functions and surface wave dispersion. *Journal of Geophysical  
464 Research: Solid Earth*, 118(1), 262-276. doi: 10.1029/2012JB009602
- 465 Tyner, G. N., & Smith, D. (1986). Peridotite xenoliths in silica-rich, potas-  
466 sic latite from the transition zone of the Colorado Plateau in north-central  
467 Arizona. *Contributions to Mineralogy and Petrology*, 94(1), 63-71. doi:  
468 10.1007/BF00371227
- 469 Valentine, G. A., & Perry, F. V. (2007). Tectonically controlled, time-predictable  
470 basaltic volcanism from a lithospheric mantle source (central Basin and Range  
471 Province, USA). *Earth and Planetary Science Letters*, 261(1), 201-216. doi:  
472 10.1016/j.epsl.2007.06.029